PARTICLE UNSTABLE EXCITED STATES IN ^{9}Be: INFLUENCE OF BETA RECOIL AND WIDTH ON DELAYED PARTICLE SPECTRA

G. Nyman[a], R.E. Azuma[b], B. Jonson[a], K.-L. Kratz[c], P.O. Larsson[d], S. Mattsson[d] and W. Ziegert[c]

a) CERN-ISOLDE, CERN, Geneva, Switzerland

b) Department of Physics, University of Toronto, Ontario, Canada

c) Institut für Kernchemie, Universität Mainz, Fed. Rep. Germany

d) Department of Physics, Chalmers University of Technology, Göteborg, Sweden

Abstract

The light nucleus ^{9}Be has been studied through the emission of beta-delayed neutrons and alpha particles from ^{9}Li. The activity was produced at the ISOLDE facility in fragmentation reactions induced either by 600 MeV proton or 910 MeV ^{3}He beams from the CERN Synchro-cyclotron. After mass separation, neutron spectra were recorded using ^{3}He-filled proportional counters, while surface barrier detectors were used for the spectroscopy of alpha particles.

Effects on the spectrum shape induced by recoil and polarization phenomena as well as large widths of the intermediate states are discussed.

1. Introduction

The nucleus ^{9}Li with a half-life[1] of $T_{\frac{1}{2}} = 178$ ms is the next heaviest lithium isotope. Its total beta-decay energy[2] is Q = 13.607 MeV. The beta decay can thus populate states, in the daughter nucleus ^{9}Be, with excitation energies which exceed the separation energies for one neutron or an alpha particle. In Fig. 1 the decay scheme[3] of ^{9}Li is shown. For the excited states in ^{9}Be fed by the beta decay, several decay channels are open such as $\alpha + {}^5\text{He} \rightarrow \alpha + \alpha + n$, $n + {}^8\text{Be} \rightarrow n + \alpha + \alpha$, and $n + {}^8\text{Be}^*(2^+) \rightarrow n + \alpha + \alpha$.

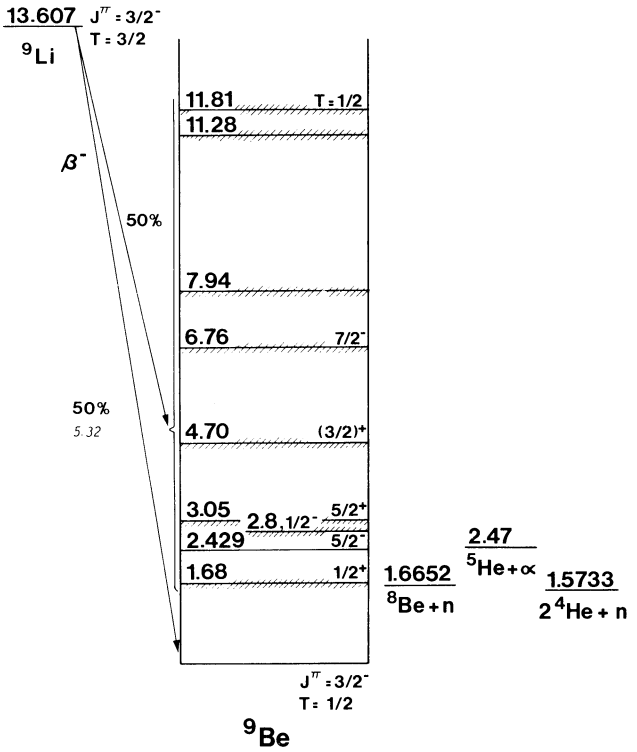

Fig. 1 The decay scheme of ^{9}Li

Table 1

Isotope	E_x (MeV ± keV)	Γ (keV)
^{9}Be	2.4294 ± 1.3	0.77 ± 0.15
	2.78 ± 120	1080 ± 110
	3.049 ± 9	282 ± 11
	4.704 ± 25	743 ± 55
	6.76 ± 60	1540 ± 200
	7.94 ± 80	∿ 1000
	11.283 ± 24	575 ± 50
	11.81 ± 20	400 ± 30
^{8}Be	ground state	(6.8 ± 1.7) × 10^{-3}
	2.94 ± 30	1560 ± 30
^{5}He	ground state	600 ± 20

Since most of the intermediate states in the decay cascade are very broad, no narrow peak structure could be expected in the spectra except for the neutron transition between the $I^\pi = \frac{5}{2}^-$ state in ^{9}Be and the ground state of ^{8}Be. In Table 1, energies[2] and widths[2] are given for all known states in the energy regions of interest.

2. Experimental technique

For the neutron spectroscopic measurements the mass-separated ion beam was brought, via an ion optical transfer line, to a measuring position situated one floor above the isotope separator in order to reduce the background level. In addition, a shielding consisting of paraffin, polyethylene, and cadmium sheets completely surrounded the neutron spectrometer. For the neutron detection, two ^{3}He-filled spectrometers were used. The energy resolution of the detectors was 14.3 keV (FWHM) for the thermal neutron peak and 30 keV (FWHM) at 500 keV.

For the alpha measurements the ^{9}Li beam was stopped in a 20 μg/cm^2 carbon foil and the sepctra were measured with either a detector telescope consisting of two silicon surface-barrier detectors or a singles detector.

3. The neutron spectrum

Figure 2 shows the measured neutron spectrum corrected for the energy dependence of the detection efficiency. The general shape of the spectrum agrees with earlier measurements by Macefield et al.[4] and Chen et al.[5], who both measured the neutron spectrum with time-of-flight techniques. The energy resolution in the present measurement is, however, superior to that reached in Refs. 4 and 5.

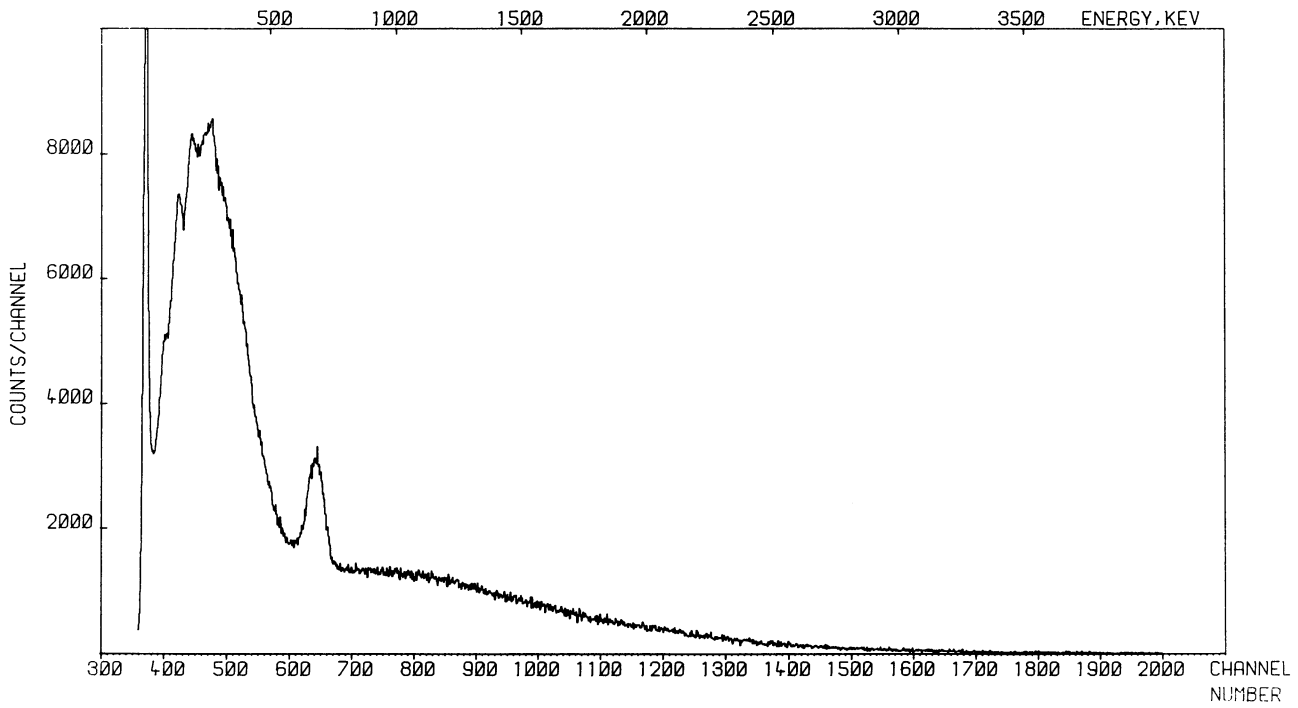

Fig. 2 Efficiency-corrected energy spectrum of beta-delayed neutrons from ^{9}Li. The spectrum was measured with a ^{3}He-filled proportional counter.

Besides the thermal-neutron peak, due to background radiation, and two broad distributions, only one peak, with energy 682 keV, can be seen in the spectrum. This peak corresponds to the neutron transition from the state ($I^{\pi} = 5/2^{-}$) at 2.43 MeV excitation energy in ^{9}Be to the ground state ($I^{\pi} = 0^{+}$) of ^{8}Be. This peak is broader than expected from either the detector resolution or the natural widths (Table 1) of the states involved. The broadening is explained[6] as a recoil effect due to i) the high beta-decay energy, ii) a light beta-decay daughter, iii) a short lifetime of the neutron-emitting state, and iv) a possible beta-decay induced polarization of the daughter product. Owing to the short lifetime (8.5×10^{-19} s) of the 2.43 MeV state in ^{9}Be, the recoiling nucleus is not retarded through collisions with neighbouring atoms before it decays by neutron emission. Depending on the angle of emission relative to the recoil direction, the neutron energy will be shifted.

The first step in the calculation of the broadened line shape is to obtain the recoil-energy distribution of the beta-decay daughter ^{9}Be*. The expression[7] for the emission probability of an electron-antineutrino pair in allowed beta decay can be transformed to describe the distribution of recoil energies as

$$P(W,E_R)\, dW\, dE_R = F(A,W)\left\{W(W_0-W) + \frac{1}{2}\alpha \times \left[2E_R \frac{M_C c^2}{m_0 c^2} - W^2 + 1 - (W_0-W)^2\right]\right\} dW\, dE_R \quad (1)$$

with F(A,W) the Fermi function, W the total electron energy, W_0 the maximum electron energy, E_R the recoil energy, M the mass of the recoiling nucleus, m_0 the rest mass of electron, and α the beta-neutrino angular correlation factor[7]. Since in this case the beta decay is of the Gamow-Teller type ($3/2^{-} \rightarrow 5/2^{-}$), α equals $-1/3$. The recoil energy distribution ranges between 0 and 8.14 keV.

For the second part of the decay cascade, the neutron emission, we make the assumption that the excited ^{9}Be nucleus consists of an ^{8}Be core surrounded by an orbiting neutron with angular momentum quantum number l = 3. The linear momentum of the recoiling ^{9}Be* nucleus is shared between the neutron and the ^{8}Be core such that

$$\vec{p}_R(n) = \vec{p}_R(^{9}\mathrm{Be}^*) - \vec{p}_R(^{8}\mathrm{Be}) \ , \quad (2)$$

where the index R stands for recoil. To obtain the total linear momentum $\vec{p}'_n$, the linear momentum $\vec{p}_n$, released in the decay, is vectorially added to $\vec{p}_R(n)$ as

$$p'^2_n = p_n^2 + p_R^2(n) + p_n p_R(n) \cos\theta_1 \quad (3)$$

which transforms to

$$E'_n(E_R,\theta_1) = E_n + \frac{1}{M(n)}\left[\frac{M(^{9}\mathrm{Be}^*) - M(^{8}\mathrm{Be})}{M(^{9}\mathrm{Be}^*)}\right]\left\{M(^{9}\mathrm{Be}^*)E_R \times \left[\frac{M(^{9}\mathrm{Be}^*) - M(^{8}\mathrm{Be})}{M(^{9}\mathrm{Be}^*)}\right] + 2\sqrt{M(^{9}\mathrm{Be}^*)M(n)E_n E_R}\cos\theta_1\right\} , \quad (4)$$

where θ_1 is the angle between the directions of recoil and neutron emission. The final neutron energy is denoted by E'_n, while E_n stands for the neutron energy in the case of a stationary nucleus. The maximum energy contribution [Eq. (4)] due to the beta recoil is about ±50 keV. If isotropic emission of neutrons is assumed, the neutron intensity distribution $P_n(E'_n,E_R)$ for fixed E_R is obtained simply from integration over solid angles corresponding to different neutron energy intervals. Finally, the neutron spectrum $N(E'_n)$ is obtained by integrating $P_n(E'_n,E_R)$, weighted by the distribution $P_R(E_R)$ of recoil energies, over E_R as

$$N(E_n')\,dE_n' = \int_{E_R} P_n(E_n',E_R)P_R(E_R)\,dE_n'\,dE_R \ . \qquad (5)$$

From Eq. (1) $P_R(E_R)$ is obtained after integration over all electron energies W.

The dashed curve in Fig. 3 shows, together with experimental data, the calculated line shape obtained with the assumption of isotropic emission of neutrons. The expected line shape in the absence of recoil effects is indicated by the dashed-dotted curve.

The precursor nucleus ^{9}Li is unoriented, but the recoiling neutron emitter possesses a distribution[8] of m-values along its direction of flight expressed by

$$P(m) = \frac{1}{2j+1}\left\{1 - (A+B)\,X_1\,\frac{m}{j} - \frac{2}{3}\,CX_2\left[\frac{j(j+1) - 3m^2}{j(2j-1)}\right]\right\} . \qquad (6)$$

Equation (6) is to be considered only as an approximation since it expresses the distribution averaged over electron energy. Evaluation of the coefficients[8,9] in Eq. (6) gives the final expression

$$P(m) = \frac{1}{2j+1}\left[1 + \frac{2}{3}\,X_2\,\frac{j(j+1) - 3m^2}{j(2j-1)}\right] , \qquad (7)$$

where X_2 is a function of the maximum kinetic energy released in the decay. We notice that only a quadratic dependence of m remains in Eq. (7). This causes nuclear alignment, which means that the magnetic substates are differently populated but in a way such that P(m) = P(-m). For this case the relative population of different substates is

$$P(\pm 1/2) = 0.2109$$
$$P(\pm 3/2) = 0.1777$$
$$P(\pm 5/2) = 0.1113 \ .$$

As a consequence of the alignment of the beta-decay daughter, the neutrons will be emitted anisotropically. In the formalism[10] for angular correlations in cascade decays we express the probability for an observation W in the final state as

$$W = \sum_{m_1}\sum_{m_2}\left|\sum_{m}(j_2m_2|H_{r_2}|jm)(jm|H_{r_1}|j_1m_1)\right|^2 , \qquad (8)$$

where 1 and 2 denote the initial and final states, respectively, and H_r is the interaction Hamiltonian. The interaction matrix element for the first part of the decay is proportional to P(m), the population of magnetic substates. The Hamiltonian in the interaction matrix element $|(j_2m_2|H_{r_2}|jm)|^2$ represents the probability for a transition from the intermediate state to the final state. Since it has to be invariant under rotations of the coordinate system, it is formed by a scalar product of two irreducible tensors as

$$H_{r2} = \sum_{J}\sum_{M}(-1)^{J-M}\,A_{J,-M}\,T_{JM} , \qquad (9)$$

both tensors being of half-integer rank $J = \frac{5}{2}$. After appropriate coordinate transformations and evaluation of vector coupling constants, the following expression for the angular dependence of the neutron emission is derived:

$$W(\theta) = 1 + 0.459\cos^2\theta \ . \qquad (10)$$

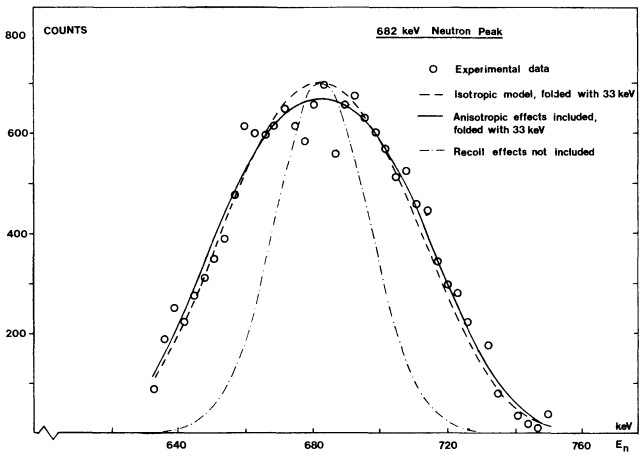

Fig. 3 Experimental and calculated shapes of the 682 keV peak in the beta-delayed neutron spectrum of ^{9}Li. The strong influence of recoil effects is evident from a comparison between the expected line shape considering only the detector resolution (dashed-dotted line) and the measured spectrum.

Thus the nuclear alignment contributes to the broadening of the line. The solid curve in Fig. 3 shows the calculated line shape when anisotropic effects are included.

4. The alpha spectrum

Figure 4 shows the ^{9}Li beta-delayed alpha-particle spectrum registered with a detector telescope. The main intensity peaks around 320 keV. This peak structure is composite due to the many decay channels open. More striking, however, is the fact that the alpha spectrum ranges to energies above 5 MeV. In the work[5] of Chen et al. no alpha intensity was found at such high energies, but recently Langevin et al.[11] found high-energy alpha particles. In the following we will concentrate on the high-energy part of the alpha spectrum, with the aim of extracting the beta feed to the highly excited states in ^{9}Be.

The alpha particles of highest energy originate in the states at 11.81 MeV and 11.28 MeV excitation energy in ^{9}Be through decay via the channel

$$^9\mathrm{Be}^* \rightarrow \alpha_1 + {}^5\mathrm{He} \ , \qquad {}^5\mathrm{He} \rightarrow \alpha_2 + n$$

Both states in ^{9}Be* as well as the ground state of ^{5}He have large widths (Table 1) which will impose considerable energy shifts for the emitted alpha particles.

The state fed in beta decay is described by a Breit-Wigner shape as

$$Y_E' = \frac{C}{(E - E_{res})^2 + \frac{1}{4}\Gamma^2} , \qquad (11)$$

where E is the excitation energy and E_{res} is the energy of the resonance in ^{9}Be. The width of the state is denoted by Γ, and C is a constant. However, owing to the Coulomb force, the beta decay populates the resonance asymmetrically. The intensity distribution of the beta feed is obtained by weighting Eq. (11) with the dimensionless integral Fermi function f(Z,Q-E) as

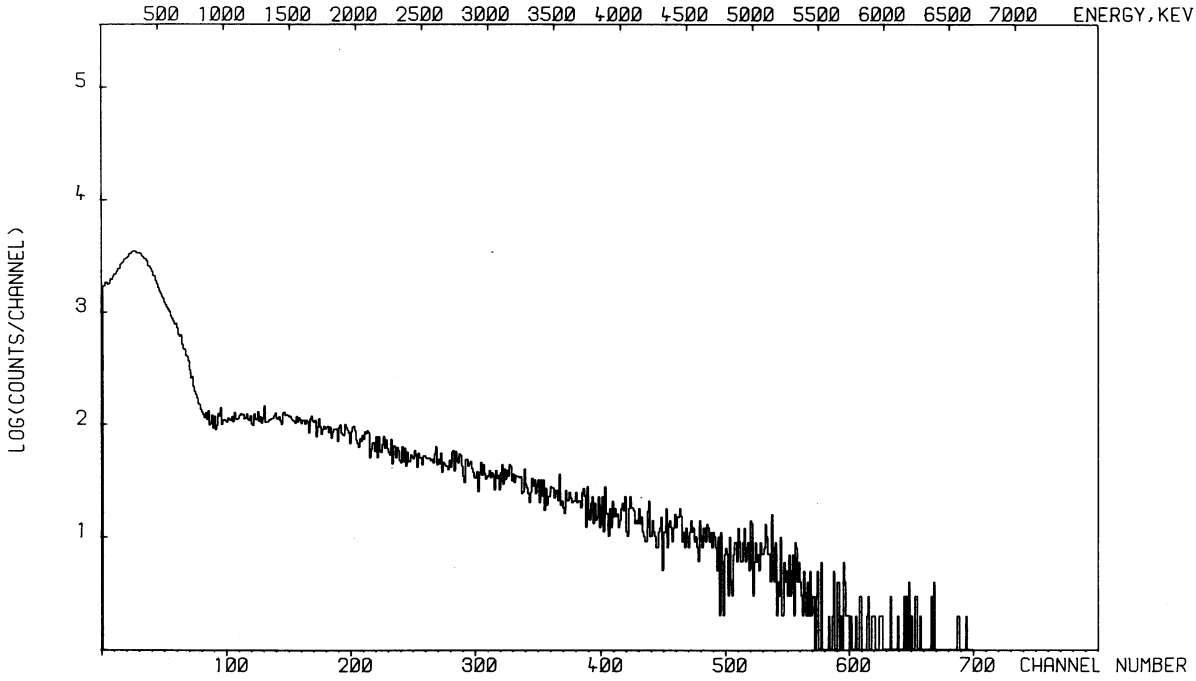

Fig. 4 Energy spectrum of beta-delayed alpha particles from ^{9}Li. The spectrum was measured with a surface-barrier detector telescope in anticoincidence mode.

$$Y_E = \frac{(Q-E)^5}{(E - E_{res})^2 + \frac{1}{4}\Gamma^2} \,. \qquad (12)$$

The function f(Z,Q-E) has been approximated with $(Q-E)^5$ in order to vizualize the very strong energy dependence. Assuming that the Breit-Wigner shape is valid, the beta feed extends, through the tail of the distribution in Eq. (12), down to the ground state of ^{5}He. This effect[12] was already shown for the decay of ^{8}He, but it is more pronounced in this case because of the high excitations involved.

The spectrum shape is obtained from an integration over the state fed in beta decay and the ground state of ^{5}He, which are split up as schematically illustrated in Fig. 5. Each of the "discrete levels" in ^{9}Be* decays by alpha emission to every accessible "discrete level" in ^{5}He. All decay paths are calculated under consideration of alpha and neutron penetrabilities. The intensity distribution of alpha particles depopulating the ^{9}Be* nucleus is finally given by

$$Y_{\alpha_1}(E_{Ii},E_{Ff}) = \qquad (13)$$

$$= \frac{(Q-E_{Ii})^5 P^{\alpha}(E_{\alpha_1}) P^{n}(E_n)}{[(E_{Ii} - E_{res}^{(I)})^2 + \frac{1}{4}\Gamma_I^2][(E_{Ff} - E_{res}^{(F)})^2 + \frac{1}{4}\Gamma_F^2]} \,,$$

where I and F denote initial and final states, and i and f are running indices. The penetrabilities P^{α} for alpha particles have been calculated according to Fröberg[13], whereas the simple formula[14] of Blatt and Weisskopf has been used for the neutron penetrabilities P^{n}. The sum of all possible decay paths finally gives the total spectrum. Spectra from the breakup of ^{5}He into an alpha particle and a neutron are calculated taking recoil effects into account in a way

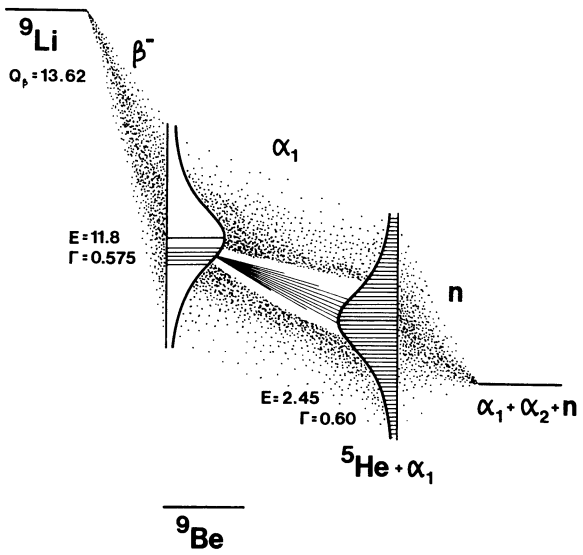

Fig. 5 Schematic illustration of the beta-delayed particle emission process through the channel

$$^{9}\mathrm{Li} \xrightarrow{\beta^-} \alpha_1 + {}^{5}\mathrm{He} \rightarrow \alpha_1 + \alpha_2 + n \,.$$

similar to that described in Section 3. Figure 6 shows the calculated alpha spectrum (solid line) from the decay of the 11.81 MeV state in ^{9}Be as well as its decomposition into partial spectra of α_1 and α_2. It is noteworthy that the spectrum covers the entire range from zero energy to above 5 MeV. This behaviour is due to the large tail, towards low energies, of the state fed in the beta decay [Eq. (12)].

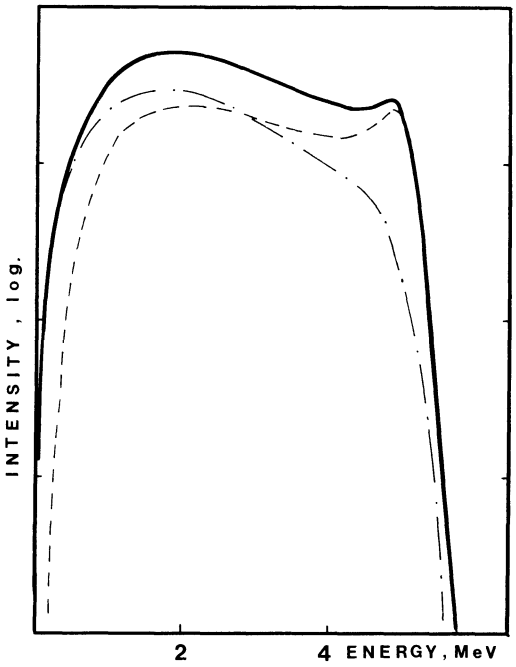

Fig. 6 Calculated alpha-particle spectrum (solid curve) from the decay of the 11.81 MeV state in ^{9}Be. The dashed and dashed-dotted curves show the decomposition into partial spectra of α_1 and α_2 (cf. Fig. 5).

Figure 7 shows a beta-delayed alpha-particle spectrum of ^{9}Li measured with a singles surface-barrier detector. Also included in the figure is the sum of calculated spectra from the states at 11.81 MeV and 11.28 MeV excitation energy in ^{9}Be. From the calculated spectrum normalized to the experimental one at the high-energy part, it is found that 6% of the intensity in the alpha spectrum originates from the 11.81 MeV state and 2.4% from the 11.28 MeV state. Since 50% of the beta decay feeds[3] particle unbound states, the beta-decay branches to

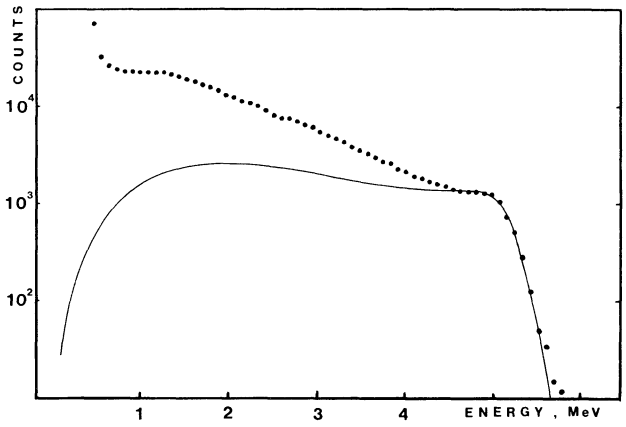

Fig. 7 Beta-delayed alpha-particle spectrum of ^{9}Li measured with a singles surface-barrier detector (filled circles). The solid curve shows the normalized calculated spectrum from the 11.81 MeV and 11.28 MeV states in ^{9}Be.

these states are 3% and 1.2%, respectively. In contradiction to Langevin et al.[11] we thus find a strong beta-decay branch to the state at 11.81 MeV in ^{9}Be. The main part of the beta feed proceeds to the tail of the state because of the strong energy dependence of the phase-space factor f(Z,Q-E) in Eq. (12). Only 23% of the beta feed to the 11.81 MeV state falls within ±2Γ of the resonance energy.

A logft value calculated in the traditional way would evidently, in this case, result in a strong underestimate. An alternative method is to deduce an average logft value by integrating the phase-space factor over the profile of the broad state. Such a procedure results in average logft values of 5.16 and 5.49 for the transitions to the 11.81 MeV and 11.28 MeV states, respectively.

REFERENCES

1) D.E. Alburger and D.H. Wilkinson, Phys. Rev. C 13 (1976) 835.

2) F. Ajzenberg-Selove, Nucl. Phys. A320 (1979) 1.

3) T. Björnstad, H.-Å. Gustafsson, P.G. Hansen, B. Jonson, V. Lindfors, S. Mattsson, A.M. Poskanzer and H.L. Ravn, Nucl. Phys. A359 (1981) 1.

4) B.E.F. Macefield, B. Wakefield and D.H. Wilkinson, Nucl. Phys. A131 (1969) 250.

5) Y.S. Chen, T.A. Tombrello and R.W. Kavanagh, Nucl. Phys. A146 (1970) 136.

6) R.D. Macfarlane, N.S. Oakey and R.J. Nicles, Phys. Lett. 34B (1971) 133.

7) C.S. Wu and S.A. Moskowski, Beta decay (Wiley, New York, 1965).

8) H. Frauenfelder, J.D. Jackson and H.W. Wyld Jr., Phys. Lett. 110 (1958) 451.

9) J.D. Jackson, S.B. Treiman and H.W. Wyld Jr., Nucl. Phys. 4 (1957) 206.

10) M.E. Rose, Elementary theory of angular momentum (Wiley, London, 1957).

11) M. Langevin, C. Détraz, D. Guillemaud, F. Naulin, M. Epherre, R. Klapisch, S.K.T. Mark, M. de Saint-Simon, C. Thibault and F. Touchard, β-delayed charged particles from ^{9}Li and ^{11}Li (to be published).

12) T. Björnstad, H.-Å. Gustafsson, B. Jonson, P.-O. Larsson, V. Lindfors, S. Mattsson, G. Nyman, A.M. Poskanzer, H.L. Ravn and D. Schardt, The decay of ^{8}He. To be published in Nucl. Phys. A.

13) C.-E. Fröberg, Rev. Mod. Phys. 27 (1965) 399.

14) J.M. Blatt and V.F. Weisskopf, Theoretical nuclear physics (Springer-Verlag, New York, 1979), p. 361.